Wiley Online Library
Early View publication on www.wileyonlinelibrary.com
(issue and page numbers not yet assigned;
citable using Digital Object Identifier – **DOI**)

Phys. Status Solidi B, 1–8 (2016) / **DOI** 10.1002/pssb.201600485

physica status solidi b
www.pss-b.com
basic solid state physics

Photoelectric and photoluminescence properties of CdTe–GaTe composite

Iuliana Caraman[1], Nicolae Spalatu[2], Igor Evtodiev[3,4], Dumitru Untila[*,3,4], Liviu Leontie[5], and Mihail Caraman[3]

[1] Engineering Department, Vasile Alecsandri University of Bacau, 157 Calea Marasesti, RO-600115 Bacau, Romania
[2] Department of Materials Science, Tallinn University of Technology, Ehitajate tee, 5, EE-19086 Tallinn, Estonia
[3] Faculty of Physics and Engineering, Moldova State University, 60 A. Mateevici, MD-2009 Chisinau, Republic of Moldova
[4] Ghitu Institute of Electronic Engineering and Nanotechnologies, Academy of Sciences of Moldova, Academiei, 3/3, MD-2028 Chisinau, Republic of Moldova
[5] Alexandru Ioan Cuza University of Iasi, Carol I, 11, RO-7 00506 Iasi, Romania

Received 29 June 2016, revised 9 September 2016, accepted 27 September 2016
Published online 14 October 2016

Keywords CdTe, composites, GaTe, photoelectric properties, photoluminescence, thermoluminescence

[*] Corresponding author: e-mail dumitru.untila@yahoo.com, Phone: +373 69 446 685, +373 22 577 589, Fax: +373 22 244 248

A GaTe–CdTe composite was obtained by thermal treatment at 1020 K of GaTe single crystals in Cd vapor atmosphere. The composite photoluminescence, photoconductivity, and composition are studied in this work. The photosensitivity and photoluminescence band structure are determined for both the primary crystals and the composite. The CdTe crystallites create, in the GaTe bandgap, recombination and trapping levels, which determine the structure of the photoluminescence spectra and the spectral range of composite photosensitivity. The photoluminescence spectrum of the composite at 80 K contains characteristic bands of both composite components, GaTe and CdTe. From the analysis of thermally stimulated luminescence curves, the energies of the electron trapping levels in the composite are determined.

© 2016 WILEY-VCH Verlag GmbH & Co. KGaA, Weinheim

1 Introduction Layered III–VI semiconductors, particularly gallium monotelluride (GaTe), exhibit special properties related to the character of optical transitions in the region of fundamental absorption threshold, marked anisotropy of physical properties, significant photoluminescence (PL), and photosensitivity in the visible and near-infrared (NIR) regions [1–3]. The GaTe is a p-type semiconductor with a direct bandgap of 1.67 eV at room temperature [4, 5]. Its single crystals are composed of layered atomic packings of Te–Ga–Ga–Te type with strong bonds of ionic-covalent type inside packings and weak van der Waals polarization bonds between them [6, 7]. Packings are so disposed to one another that cracks are formed between them, in which atoms and molecules can easily intercalate [8–16]. The van der Waals planes are free of dangling bonds and prove to be very inert to chemical reactions [17].

Thanks to its properties, gallium telluride is considered a promising material for solar energy applications [18–21]. A special attention is paid to study of electric and optical properties, as well as energy band structure of Te compounds with Ga, due to the perspective of their use as base material in ionizing radiation receivers, thermoelectric devices, electronic memory elements, and as solid electrolytes [1, 22–26].

Both the low electric conductivity and presence of heavy atoms (Te) in the composite's lattice determine the stability to ionizing radiation of GaTe-based photoelectric devices and allow the possibility to use it in radiation detectors [24–27]. The weak bonds between elementary GaTe packings facilitate crystal cleavage in plan-parallel single crystalline lamellas (plates) with a low surface state density. Plate thickness can vary from tens of nanometers up to millimeter range. These properties stimulate research toward obtaining wideband sensitivity photoreceivers [28, 29].

Cadmium telluride (CdTe) has an energy bandgap which correlates well with the maximum conversion efficiency of a photovoltaic device. At the same time, Cd and Te heavy elements are present in this compound. These properties make CdTe a promising candidate for use in photoelectronics and ionizing radiation detectors [30, 31].

© 2016 WILEY-VCH Verlag GmbH & Co. KGaA, Weinheim

Due to the aforementioned considerations, the GaTe–CdTe composite can be considered, in turn, as an important material for photoelectronics and ionizing radiation detectors.

In this work, structural, photoelectric, and PL properties of the GaTe–CdTe composite obtained by annealing of GaTe plates in Cd vapors are studied.

2 Experimental The GaTe single crystals used as the base material were grown by vertical Bridgman–Stockbarger technique [32]. The primary compound was synthesized from Ga (5N) and Te (5N) elementary components, taken in stoichiometric proportions. As obtained GaTe single crystals were of p-type, with a hole concentration of $(1.5–4.0) \times 10^{15}\,cm^{-3}$ at 293 K.

The GaTe–CdTe composite was obtained as follows. From massive single crystals plates with natural surfaces of $8 \times 10\,mm^2$ and thicknesses from 30 μm up to 500 μm have been cleaved. These were introduced into quartz ampoules with an internal diameter of 12–15 mm. In one of ampoule, a quantity of $2\,mg\,cm^{-3}$ Cd was introduced. After air evacuation to 1.5×10^{-5} Torr, the ampoules were sealed and introduced in a furnace, at a temperature of 1020 K. At this temperature, the pressure of Cd vapor represents ~1 Torr.

In order to evaluate the crystal structure of the compounds, X-ray diffraction (XRD) studies were carried out with an Empyrean (PANanalytical) X-ray diffractometer, using $CuK_{\alpha 1}$ radiation ($\lambda_{CuK\alpha 1} = 0.154060$ nm). The photoluminescence of GaTe plates and GaTe–CdTe composite was excited using a He–Ne laser ($\lambda = 632.8$ nm). The power density could be varied in the range of $0.1–4\,kW\,cm^{-2}$ using neutral filters. The samples temperature during PL recording was measured with a T-type thermocouple, in the range from 78 to 300 K. The PL spectra were recorded by a spectrophotometric equipment based on an MDR-2 type monochromator with a diffraction grating ($600\,mm^{-1}$), the overall energy resolution of which was of ~1 meV.

For photoconductivity (PC) measurements in transversal geometry (the incident radiation direction and current direction are reciprocally perpendicular) (Fig. 1a) from both GaTe and GaTe–CdTe plates parallelepiped-shaped samples were cut with a surface area of $6 \times 4\,mm^2$ and thickness of ~30 μm. Thin In layers, used as electrodes, were deposited by thermal evaporation under vacuum ($\sim 5 \times 10^{-6}$ Torr). The samples used for PC measurements in longitudinal geometry (the incident radiation direction and current direction are parallel) were obtained by cleavage of GaTe–CdTe composite plates with a thickness of ~500 μm. Parallelepipedic samples with $6 \times 4\,mm^2$ base area and thickness of 200–300 μm have been thus obtained. Thin optically transparent In_2O_3 layers were then deposited and served as electrodes (Fig. 1b). After electrode deposition, the samples were annealed for 1 h in vacuum, at 420–450 K.

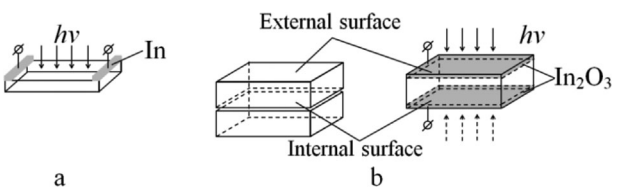


Figure 1 Sample geometry for photoconductivity measurements: (a) transversal geometry and (b) longitudinal geometry.

3 Results and discussion The XRD patterns of the GaTe single crystals and GaTe–CdTe composite obtained by thermal treatment, for 24 h, of GaTe plates in Cd vapors, at 1020 K, are presented in Fig. 2a and b, respectively.

As can be observed from Fig. 2, XRD pattern of GaTe–CdTe composite contain both diffraction lines characteristic to GaTe [with Miller indices (−6 0 1), (3 1 0), (−6 0 3), (−9 1 3), (0 0 4), also present in the pattern of pure GaTe (Fig. 2a)], and CdTe [with Miller indices (1 1 1), (2 2 2), (2 2 0), (3 3 1), (5 1 1)]. At 2θ angles of 23.8, 39.3, 45.4, and 71.2°, the diffraction lines characteristic to CdTe and GaTe are overlapped, leading to increased relative intensities. Presence of CdTe crystallites in the composite is well emphasized by the reflections located at 2θ angles of 62.32 and 72.16° (Fig. 2b).

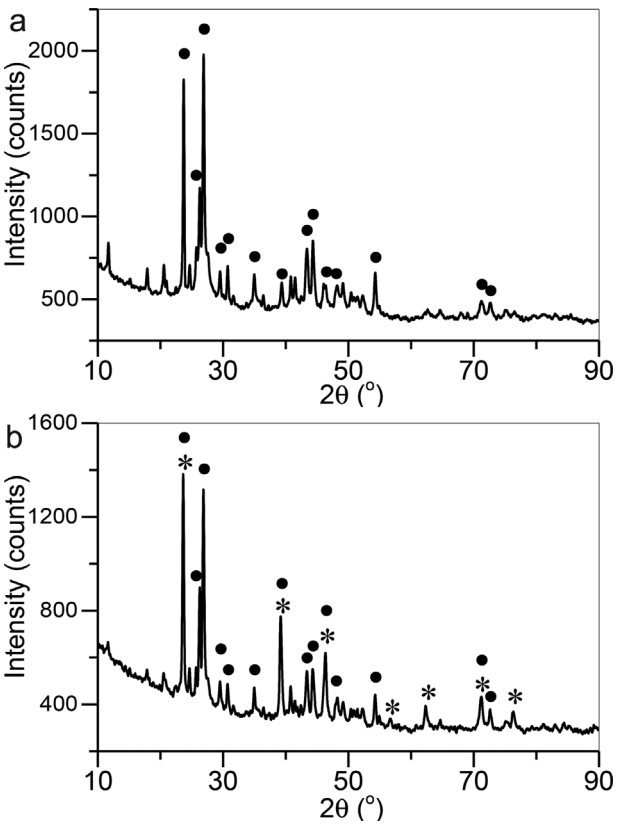


Figure 2 XRD patterns of the GaTe crystals (a) and GaTe–CdTe composite (b). ● – GaTe, PDF card no.: 01-074-8974; ✻ – CdTe, PDF card no.: 01-070-8043.

© 2016 WILEY-VCH Verlag GmbH & Co. KGaA, Weinheim

From the comparison of XRD patterns of the composite obtained at 833 K, presented in one of our earlier papers [33], and actual XRD pattern (Fig. 2b), it can be seen that an increased annealing temperature leads to an increase in the physical widening of diffraction lines, indicating a decrease of the crystallite sizes for the composite.

Figure 3 shows spectral distributions of photocurrent density, Σ (SDPD) in transversal geometry (Fig. 1a) for single crystalline GaTe (curve 1) and GaTe–CdTe composite (curve 2), and longitudinal geometry (Fig. 1b) for GaTe–CdTe composite, illuminated on external surface (curve 3) and internal surface (curve 4).

The edge of photosensitivity band, at room temperature, of GaTe single crystals (Fig. 3, curve 1), measured in transversal geometry, corresponds to absorption threshold of this compound (Fig. 3, inset). The photosensitivity edge in the photon energy region of 1.61–1.68 eV is determined by the presence of exciton absorption and absorption continuum. Since the binding energy of the electron–hole pair (16 meV [32]) is smaller than thermal energy at room temperature (kT ≈ 25 meV), excitons in GaTe are partially ionized. The slow increase of photocurrent density together with photon energy in the spectral range from 1.7 eV up to 3.2 eV is related to the increase of absorption coefficient in the *P* point of the Brillouin zone (optical band-to-band transitions) [35]. The decrease of photocurrent density for photon energy $h\nu > 3.2$ eV can be caused by a more pronounced increase of absorption coefficient in this spectral region [36, 37]. In this region, the absorption coefficient is determined by the optical transitions not only in the *P* point, but also in other high symmetry points of Brillouin zone, such as *Z* point.

The spectral dependence of photocurrent density (divided by the number of incident photons) is given by the following formula [1]:

$$\Sigma \sim A\left(1 - \frac{SL}{D}\frac{\coth\frac{d}{2L} - \alpha L \coth\frac{\alpha d}{2}}{1-\alpha^2 L^2}\right), \tag{1}$$

where *A* is a coefficient which determines the density of photons in the beam absorbed by the sample, *S* recombination rate, *D* ambipolar diffusion coefficient, *L* mean free path of nonequilibrium charge carriers, *α* absorption coefficient. For a plate thicknesses *d* that satisfies the inequality $\alpha d \gg 1$, the photosensitivity is directly proportional to recombination rate at the non-illuminated surface and it is inversely proportional to the absorption coefficient:

$$\Sigma \sim 1 + \frac{S}{D}\frac{L}{1+\alpha L}. \tag{2}$$

The absorption coefficient increasing together with photon energy leads to a decreased thickness of the layer within which generation of nonequilibrium charge carriers occurs and also to the increase of the recombination rate through surface states.

The SDPD characteristic of GaTe–CdTe sample, with thickness of 30 μm, measured in transversal geometry, is presented in Fig. 3, curve 2. As can be inferred from here, the SDPD edge of the composite is shifted toward lower energies compared to that of GaTe. This shift can be due to the recombination processes through impurity levels of the GaTe crystallites from the composite.

The maximum of SDPD curve for GaTe–CdTe composite, measured in transversal geometry, is also found in the absorption band depth of the crystallites from the composite (∼1.9 eV) (Fig. 3, curve 2). The photosensitivity band edge of these samples exhibits a red-shift with respect to the absorption threshold of GaTe crystals and it is located in the immediate vicinity of absorption band edge of CdTe crystals (1.5 eV [38]). Thus, it can be admitted that photoconductivity of GaTe–CdTe composite is determined by the generation-recombination processes of the nonequilibrium charge carriers in the composite crystallites.

In Fig. 3, curve 3, SDPD of GaTe–CdTe composite, measured in longitudinal geometry at illumination through internal sample surface is presented. As can be observed, the edge of SDPD is located in the vicinity of fundamental absorption band edge of CdTe (1.5 eV [38]). The photosensitivity decrease at energies over 2.4 eV (Fig. 3, curve 3) indicates a mean free path of charge carriers in GaTe crystals shorter than $1/\alpha$, for this spectral range.

The SDPD characteristic of GaTe–CdTe composite, measured in longitudinal geometry at illumination performed through external sample surface, is presented in Fig. 3, curve 4. The maximal photosensitivity of these samples is found in the region of absorption threshold of GaTe. Further, an abrupt decrease of the photocurrent occurs. This decrease indicates the presence of energy states through which recombination of nonequilibrium charge carriers occurs. Such states can be present at the CdTe/GaTe

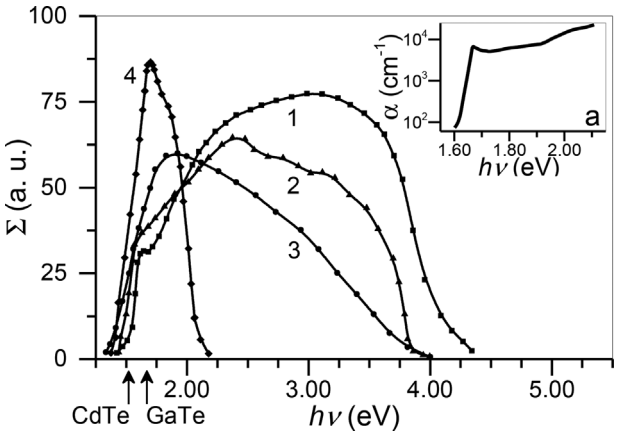


Figure 3 Spectral distributions of photocurrent in transversal geometry, for GaTe (curve 1) and GaTe–CdTe composite (curve 2), and in longitudinal geometry, for GaTe–CdTe composite, illuminated on external surface (curve 3) and internal surface (curve 4). Inset: absorption band of GaTe single crystals at room temperature [34].

© 2016 WILEY-VCH Verlag GmbH & Co. KGaA, Weinheim

crystallite interface, as well in inclusions and dislocations created by Cd atoms inserted in GaTe crystals. The presence of these defects was demonstrated for Cd-doped GaTe in the paper [39].

The PL spectra of GaTe plate, at 78 K, for excitation levels of 0.25 and 2.5 kW cm^{-2}, contain a narrow band with maximum at 1.771 eV and a low-intensity band, with maximum at ~1.68 eV (Fig. 4a). The maximum position of dominant PL band coincides with that of the absorption line of $n = 1$ direct excitons, at 80 K [34], and can be considered as radiative annihilation of free excitons. The absorption peak, at room temperature, of the $n = 1$ exciton band is found at 1.662 ± 0.002 eV. The excitonic Rydberg, determined from the absorption spectrum of GaTe at 80 K, is of 19 meV [40]. Thus, the energy bandgap values of studied GaTe single crystals are 1.681 ± 0.002 and 1.790 ± 0.002 eV at 300 and 80 K, respectively. These results are in good agreement with those published in Refs. [2, 3, 41]. The broad PL bands present in the energy region below excitonic emission band position were analyzed in Refs. [42, 43]. In these works, a donor–acceptor (DA) nature of the PL bands from the spectral range 1.4–1.7 eV was established.

As can be seen from Fig. 4a, when excitation increases by 10 times, from 0.25 kW cm^{-2} up to ~2.5 kW cm^{-2}, the intensity of this band increases according to a power function:

$$L \sim P^{\alpha}, \tag{3}$$

where power coefficient α is about 0.8, a value which is characteristic to DA emission bands [44]. Analogously, we can consider that the band with maximum at 1.684 eV represents the recombination of the pair formed by the donor of energy 0.030 eV [45], and the acceptor with energy of 75 meV. We mention that the presence of the acceptor level with energy of 74 meV was established from the measurements of the electric conductivity and Hall effect in GaTe crystals grown by Bridgman–Stockbarger method, since in the crystals grown from vapor phase an acceptor level located at 152 meV above the valence band is present [46].

The structure of PL spectrum of GaTe changes as a result of thermal treatment, for 4 h, in vacuum at 1070 K (Fig. 4b). The emission band of free excitons (FE) is strongly attenuated and is located at 1.771 eV. At the same time, two bands with maxima at 1.755 and 1.740 eV are registered.

The PL band at 1.740 eV has a full width at half maximum (FWHM) of ~12 meV, a value comparable with FWHM of FE emission in untreated GaTe (Fig. 4a). The PL

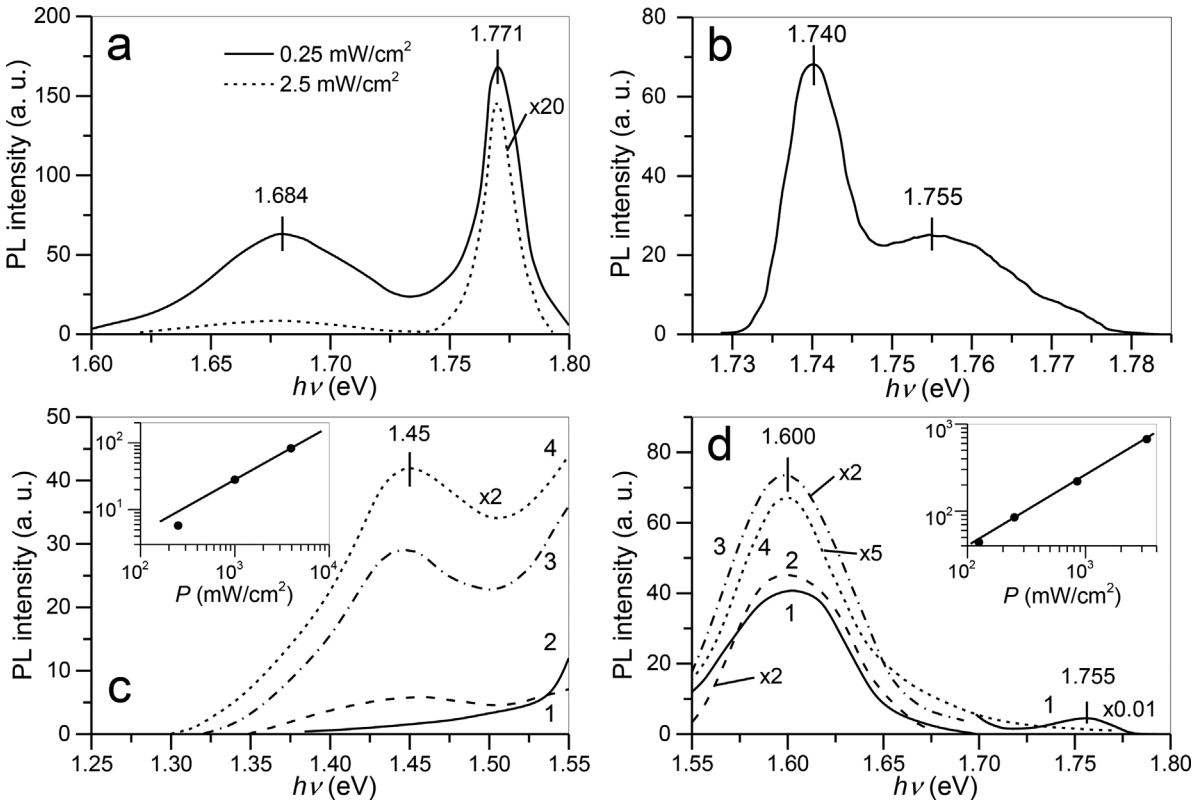


Figure 4 PL spectra, at 80 K, of GaTe single crystals (a) ($p = 0.25$ and 2.5 kW cm^{-2}), GaTe crystals annealed for 4 h in vacuum at 1070 K (b) ($p = 0.25$ kW cm^{-2}), and GaTe–CdTe composite (c and d) [$p = 0.125$ kW cm^{-2} (curve 1), 0.25 kW cm^{-2} (curve 2), 0.85 kW cm^{-2} (curve 3), and 3.3 kW cm^{-2} (curve 4)].

© 2016 WILEY-VCH Verlag GmbH & Co. KGaA, Weinheim

bands with such FWHM are characteristic to radiative exciton emission and emission processes involving excitons, which can be longitudinal optical (LO) phonon repetitions of FE or localized excitons at neutral or ionized centers.

As was demonstrated in Refs. [42, 47], the optical phonons of energy 14–23 meV participate in PL band formation in GaTe. Since the energy difference between positions of free exciton PL band and PL band at 1.740 eV is 31 meV and this value is higher than optical phonon energy, we may consider that this band represents radiative emission of localized excitons, binding energy to impurity center of which is equal to 31 meV. The luminescent emission bands of localized excitons in GaTe single crystals at temperature 10 K have been studied in Ref. [48]. This paper demonstrates that PL band at 1.73 eV represents radiative annihilation of acceptor bound excitons with binding energy of ~38 meV.

The particularity emphasized at 1.755 eV can be also considered as being of excitonic nature, namely as radiative emission of excitons bound to lattice defects in GaTe crystals annealed at high temperature (1020 K). In Refs. [49, 50], the influence of defects formed in GaTe crystals annealed at temperatures much lower than the solidification temperature, on the structure of both PL spectra and deep level diagram was studied. Short time annealing (~1 h) at 470 and 670 K lead to the attenuation of localized exciton PL and engender new donor and acceptor levels, as well as deep levels through which radiative emission occurs in the NIR spectral region.

Thermal treatment of gallium chalcogenides leads to major structural changes, with new phase formation, which modifies nut only the energy band diagram within the bandgap, but the band diagram in general [51, 52]. As was established in Ref. [50], high temperature (670 K) thermal treatment of GaTe single crystals leads to formation of both structural defects and deep energy states, which influence the generation-recombination mechanisms of nonequilibrium charge carriers in this material.

The PL spectrum, at 80 K, of GaTe–CdTe composite, for an excitation power density of ~125 mW cm^{-2}, is presented in Fig. 4c and d, curve 1. As can be seen, a complex intense band, located at 1.608 eV, which lies up to ~1.37 eV, and a low-intensity band at 1.755 eV are emphasized in the PL spectrum. The second band was also observed in the PL spectrum of GaTe crystals, thermally annealed in vacuum at ~1020 K (Fig. 4b).

The PL band with maximum at 1.600 eV covers the spectral range where both the impurity band in undoped GaTe crystals and free and localized exciton emission bands in CdTe are present [53]. The forbidden bandwidth of CdTe crystals, at 80 K, is 1.595 eV [54] and the excitonic Rydberg at 77 K is ~10 meV [55]. The latter energy is comparable with thermal energy. This fact leads to a strong attenuation of excitonic emission and also amplifies the intensity of the PL impurity band (at 1.600 eV). Since at 80 K this band covers an energy range within the absorption band of GaTe, its presence can be determined by the luminescent recombination mechanism in GaTe crystallites of the composite. To determine the nature of this band, the dependence of its PL intensity (L) on the excitation power density was analyzed (Fig. 4d, Inset). At increased excitation power density from 125 mW cm^{-2} up to 250 mW cm^{-2}, in the low energy region a new band peaked at 1.45 eV appears. The intensity of the PL bands at 1.600 and 1.450 eV increases with increasing excitation power density (P). This increase is well described with the power function (3). As can be observed from Fig. 4c, inset, the power coefficient α is 0.80 and 0.82 for the bands located at 1.600 and 1.450 eV, respectively. In Ref. [44] was shown that power coefficient values $\alpha < 1$ are characteristic to PL bands of DA type. The impurity nature of PL band with maximum at 1.600 eV is demonstrated by PL measurements of GaTe crystals at 10 K [40, 56] and $T \geq 97$ K [42]. The presence of both Ga vacancies and uncontrollable impurities contributes to the formation of two acceptor levels in GaTe, positioned at 110 and 150 meV above the valence band top, and one donor level at 75 meV below the bottom of conduction band [48]. If we take into account that the GaTe bandgap, at 80 K, is equal to 1.790 eV, then the PL band of the GaTe–CdTe composite at 1.608 eV can be interpreted as DA radiative recombination with the participation of a donor level with energy of 75 meV and an acceptor level located at 110 meV above the valence band of GaTe crystals from the composite.

The band with the maximum at 1.45 eV it is difficult to be interpreted as luminescent recombination of electrons from the conduction band holes on the acceptor level. In Refs. [45, 48], energies of donor levels of 30 and 75 meV, and acceptor levels of 110 and 150 meV have been determined. The studies reported in Refs. [57, 58] demonstrate that PL band with maximum at ~1.4 eV has an impurity nature and can be interpreted as DA radiative transition in the complex ($V_{Cd}D$).

Whereas the formation process of GaTe–CdTe composite occurs at high temperatures (1020 K), then the formation of $Cd_xGa_{1-x}Te$ solid solutions with luminescent properties is possible. In Ref. [59], the cathodoluminescence (CL) of the solid solution obtained by annealing at 1010 K of the mixture consisting of CdTe and small amounts of GaTe (concentrations <0.2 mol.%). The CL spectrum, at 78 K, of the solid solution with 0.05 mol.% GaTe contains two bands with maxima at 1.560 and 1.420 eV. The band peaked at 1.560 eV attenuates with increasing GaTe concentration and disappears at a concentration of 0.2 mol.% GaTe. Besides, a shift of the PL band located at 1.420 eV up to 1.400 eV occurs in the case of solid solution with 0.23 mol.% GaTe. At high GaTe concentrations, a mixture of two GaTe and CdTe phases is obtained. As can be inferred from Fig. 4c and d, the energy positions of PL bands of GaTe–CdTe composite do not coincide with those of CL bands of the GaTe–CdTe solid solutions.

© 2016 WILEY-VCH Verlag GmbH & Co. KGaA, Weinheim

As was demonstrated in Ref. [60], Te vacancies induce in the CdTe bandgap a donor level located at 0.04 eV below the conduction band, while Cd defects engender acceptor levels situated at 0.115 eV above the valence band. Taking into account that the bandgap of CdTe, at 80 K, is equal to 1.605 ± 0.002 eV, then the PL band with the maximum at 1.450 eV can be considered as an electronic transition between the donor level (V_{Te}) and acceptor level (Cd_{Te} defect). As a confirmation of this conclusion contributes dependence of PL intensity of the band at 1.45 eV on the excitation power density (Fig. 4, inset), which can be described by a power law (3), with a power coefficient $\alpha = 0.82$.

From the above-mentioned results, one can state that in formation of PL impurity bands of GaTe–CdTe composite (bands at 1.608 and 1.450 eV) deep acceptor levels with mean energy of ~110 meV are involved. At the same time, as experiments indicated, the luminescence quenching time is of ~5 min, which indicates that deep electron and hole trap levels are involved in the PL process. The energies of these levels have been determined from the thermally stimulated luminescence (TSL) analysis. The TSL excitation was performed with a radiation corresponding to the fundamental absorption region of GaTe single crystals. In Fig. 5, the TSL curve of the GaTe–CdTe composite, recorded after ~5 min from excitation interruption is presented. As can be seen from the PL spectra (Fig. 4c and d), the share of the band at 1.45 eV in the total PL intensity of the composite does not exceed 10%. Thus we can admit that TSL is generated in GaTe crystallites from the composite, and PL of the CdTe crystallites affects the shape of TSL curves. As can be observed from Fig. 5, the TSL contour has a complex shape that consists of several TSL elementary curves. Neglecting the repeated trapping, the initial portion of TSL curve can be described by the following formula [61]:

$$L(T) = L(T_0)\exp\left(-\frac{E_T}{kT}\right), \tag{4}$$

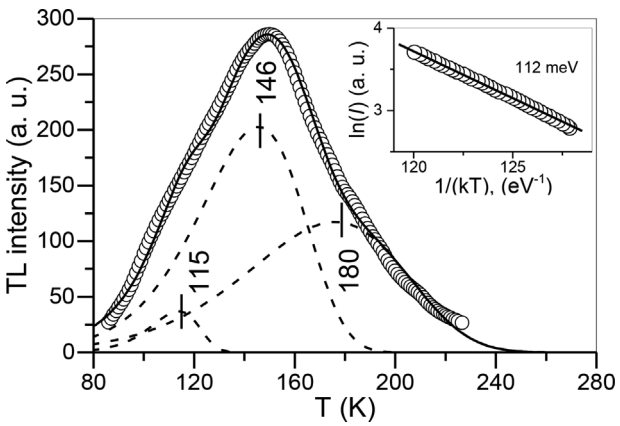


Figure 5 TSL curve of GaTe–CdTe composite.

where E_T represents the trap level energy, $L(T_0)$ luminescence signal at initial temperature (T_0), k Boltzmann constant. The dependence of TSL intensity on the reciprocal temperature, in the temperature range 84–111 K, is presented in Fig. 5, inset. From this dependence, the capture level energy was determined and found to be ~112 meV, a value which is well correlated with energy of the acceptor level involved in formation of PL band (at 1.605 eV) of GaTe–CdTe composite.

In order to determine the energies of trap levels which determine the shape of TSL curve, its contour was deconvoluted in elementary Randall–Wilkins curves [62], according to:

$$I(T) = I_M \exp\left[1 + \frac{E}{kT}\frac{T - T_M}{T_M} - \frac{T^2}{T_M^2}\left(1 - \frac{T_M}{E}\right)\right.$$

$$\left.\times \exp\left(\frac{E}{kT}\frac{T - T_M}{T_M}\right) - \frac{2kT_M}{E}\right]. \tag{5}$$

As can be observed from Fig. 5, the TSL curve of the GaTe–CdTe composite can be obtained by summation of three contours of type (5) with maxima at temperatures 113, 146, and 176 K. The approximate values of trap level energies were determined using Urbach relation [63]

$$E_t = 25kT_m, \tag{6}$$

where T_m is the temperature corresponding to the peak on TSL curve. Thus values of 0.25, 0.32, and 0.39 eV have been obtained. The trap level energies of 0.28 and 0.40 eV in GaTe single crystals have been determined by deep level transient spectroscopy [64, 65].

4 Conclusions By thermal treatment of GaTe single crystals in Cd vapor atmosphere, at temperature of 1020 K, a material composed of CdTe and GaTe crystallites (presence of which is emphasized by XRD analysis) can be obtained. The GaTe–CdTe composite exhibits promising photoelectric and photoluminescent properties in both visible and NIR ranges. The photosensitivity of GaTe–CdTe composite is determined by the concentration of both surface states and structural defects formed in the GaTe single crystals, annealed in Cd vapors. From the analysis of PL spectra and TSL curve, the exciton binding energy in GaTe crystallites from the composite, as well as energies of donor, acceptor, and capture levels have been determined.

Acknowledgements This work was financially supported by Moldova State University through the Institutional grant no. 15.817.02.34A; by the Estonian Ministry of Education and Research [IUT19-4], the European Regional Development Fund project: TK141 Centre of Excellence "Advanced materials and high-technology devices for sustainable energetics, sensorics and nanoelectronics" (1.01.2015–1.03.2023). One of the authors

© 2016 WILEY-VCH Verlag GmbH & Co. KGaA, Weinheim

(D. Untila) would like to thank the European Commission for financial support through Erasmus+ Programme.

References

[1] D. Olguin, A. Rubio-Ponce, and A. Cantarero, Eur. Phys. J. B **86**, 350 (2013).
[2] S. Pal and D. N. Bose, Solid State Commun. **97**, 725 (1996).
[3] J. F. Sanchez-Royo, A. Segura, and V. Munoz, Phys. Status Solidi A **151**, 257 (1995).
[4] K. Cinar, Z. Caldiran, C. Coskun, and S. Aydogan, Thin Solid Films **55**, 40 (2014).
[5] N. N. Kolesnikov, E. B. Borisenko, D. N. Borisenko, and A. V. Timonina, J. Cryst. Growth **365**, 59 (2013).
[6] P. Fielding, G. Fischer, and E. Mooser, J. Phys. Chem. Solids **8**, 434 (1959).
[7] W. B. Pearson, Acta Crystallogr. **17**, 1 (1964).
[8] K. Allakhverdiev, S. Hanna, A. Kulibekov, S. Ozbek, E. Gunay, and D. Huseinova, Int. J. Infrared Millim. Waves **26**, 1741 (2005).
[9] I. Caraman, E. Vatavu, L. Leontie, M. Stamate, and D. Untila, Phys. Status Solidi C **12**, 70 (2015).
[10] I. Caraman, D. Rusu, E. Ardeleanu, and I. Evtodiev, J. Optoelectron. Biomed. Mater. **7**, 27 (2015).
[11] D. Untila, V. Cantser, M. Caraman, I. Evtodiev, L. Leontie, and L. Dmitroglo, Phys. Status Solidi C **12**, 65 (2015).
[12] C. M. Julien, Mater. Sci. Eng. R **40**, 47 (2003).
[13] Y. I. Zhirko, I. P. Zharkov, Z. D. Kovalyuk, and M. M. Pyrlja, Semicond. Phys. Quantum Electron. Optoelectron. **7**, 404 (2004).
[14] Z. D. Kovalyuk, M. M. Pyrlya, and V. B. Boledzyuk, J. Optoelectron. Adv. Mater. **5**, 869 (2003).
[15] D. Untila, I. Caraman, I. Evtodiev, V. Cantser, N. Spalatu, L. Leontie, L. Dmitroglo, and E. Luchian, Energy Proc. **84**, 149 (2015).
[16] N. Spalatu, I. Evtodiev, I. Caraman, S. Evtodiev, I. Rotaru, M. Caraman, and D. Untila, Energy Proc. **84**, 176 (2015).
[17] O. Lang, R. Schlaf, Y. Tomm, C. Pettenkofer, and W. Jaegermann, J. Appl. Phys. **75**, 7805 (1994).
[18] Z. Wang, K. Xu, Y. Li, X. Zhan, M. Safdar, Q. Wang, F. Wang, and J. He, ACS Nano **8**, 4859 (2014).
[19] F. Liu, H. Shimotani, H. Shang, T. Kanagasekaran, V. Zolyomi, N. Drummond, V. I. Fal'ko, and K. Tanigaki, ACS Nano **8**, 752 (2014).
[20] P. Hu, J. Zhang, M. Yoon, X. F. Qiao, X. Zhang, W. Feng, P. Tan, W. Zheng, J. Liu, X. Wang, and J. C. Idrobo, Nano Res. **7**, 694 (2014).
[21] E. Bucher, in: Photoelectrochemistry and Photovoltaics of Layered Semiconductors, edited by A. Aruchamy (Kluwer Academic Publishers, Dordrecht, 1992), pp. 1–81.
[22] M. Balkanski, C. Julien, and J. Y. Emery, J. Power Sources **26**, 615 (1989).
[23] M. M. Nassary, Turk. J. Phys. **30**, 95 (2006).
[24] C. Rocha Leao and V. Lordi, Phys. Rev. B **84**, 165206 (2011).
[25] A. J. Nelson, A. M. Conway, B. W. Sturm, E. M. Behymer, C. E. Reinhardt, R. J. Nikolic, S. A. Payne, G. Pabst, and K. C. Mandal, J. Appl. Phys. **106**, 023717 (2009).
[26] P. M. Reshmi, A. G. Kunjomana, K. A. Chandrasekharan, M. Meena, and C. K. Mahadevan, Int. J. Soft Comput. Eng. **1**, 228 (2011).
[27] K. C. Mandal, R. M. Krishna, T. C. Hayes, P. G. Muzykov, S. Das, T. S. Sudarshan, and S. Ma, IEEE Trans. Nucl. Sci. **58**, 1981 (2011).
[28] V. N. Katerinchuk and M. Z. Kovalyuk, Tech. Phys. Lett. **25**, 54 (1999).
[29] V. N. Katerynchuk, Z. R. Kudrynskyi, and Z. D. Kovalyuk, Semiconductors **49**, 600 (2015).
[30] D. L. Bätzner, A. Romeo, H. Zogg, R. Wendt, and A. N. Tiwari, Thin Solid Films **387**, 151 (2001).
[31] K. Zuber, Phys. Lett. B **519**, 1 (2001).
[32] G. Dhanaraj, K. Byrappa, V. Prasad, and M. Dudley (Eds.), Springer Handbook of Crystal Growth (Springer, Heidelberg, 2010), p. 1816.
[33] I. Caraman, D. Untila, I. Evtodiev, V. Kantser, N. Spalatu, D. Rusu, E. Luchian, and I. Rotaru, Chalcogenide Lett. **12**, 683 (2015).
[34] V. I. Gramatsky, M. I. Karaman, and V. P. Mushinsky, Phys. Tech. Semicond. **6**, 550 (1972) (in Russian).
[35] A. Yamamoto, A. Syouji, T. Goto, E. Kulatov, K. Ohno, Y. Kawazoe, K. Uchida, and N. Miura, Phys. Rev. B **64**, 035210 (2001).
[36] V. Grasso, G. Mondio, M. A. Pirrone, and G. Saitta, J. Phys. C: Solid State Phys. **8**, 80 (1975).
[37] G. Leveque, J. Phys. C: Solid State Phys. **10**, 4645 (1977).
[38] P. Horodysky and P. Hlidek, Phys. Status Solidi B **243**, 494 (2006).
[39] B. Gürbulak, M. Şata, A. Ashkhasi, S. Duman, and G. Turgut, Int. J. Thales Eng. Sci. **2**, 12 (2016).
[40] A. Zubiaga, J. A. Garcia, F. Plazaola, V. Munoz-Sanjose, and C. Martinez-Tomas, Phys. Rev. B **68**, 245202 (2003).
[41] J. Camassel, P. Merle, H. Mathieu, and A. Gouskov, Phys. Rev. B **19**, 1060 (1979).
[42] S. Shigetomi, T. Ikari, and H. Nishimura, J. Lumin. **78**, 117 (1998).
[43] H. S. Güder, B. Abay, H. Efeoğlu, and Y. K. Yoğurtçu, J. Lumin. **93**, 243 (2001).
[44] T. Schmidt, K. Lischka, and W. Zulehner, Phys. Rev. B **45**, 8989 (1992).
[45] Zs. Rak, S. D. Mahanti, K. C. Mandal, and N. C. Fernelius, J. Phys.: Condens. Matter **21**, 015504 (2009).
[46] C. Manfredotti, R. Murri, A. Rizzo, L. Vasanelli, and G. Micocci, Phys. Status Solidi A **29**, 475 (1975).
[47] J. Z. Wan, J. L. Brebner, R. Leonelli, G. Zhao, and J. T. Graham, Phys. Rev. B **48**, 5197 (1993).
[48] A. Zubiaga, J. A. Garcia, F. Plazaola, V. Munoz-Sanjose, and M. C. Martinez-Tomas, J. Appl. Phys. **92**, 7330 (2002).
[49] A. Zubiaga, J. A. Garcia, F. Plazaola, V. Munoz-Sanjose, and M. C. Martinez-Tomas, Jpn. J. Appl. Phys. **47**, 8719 (2008).
[50] S. Shigetomi, T. Ikari, and H. Nakashima, Jpn. J. Appl. Phys. **37**, 3282 (1998).
[51] A. A. Al-Ghamdi, S. A. Khan, S. Al-Heniti, F. A. Al-Agel, and M. Zulfequar, Curr. Appl. Phys. **11**, 315 (2011).
[52] E. Filippo, T. Siciliano, A. Genga, G. Micocci, M. Siciliano, and A. Tepore, Appl. Surf. Sci. **261**, 454 (2012).
[53] S. Vatavu, H. Zhao, V. Padma, R. Rudaraju, D. L. Morel, P. Gaşin, Iu. Caraman, and C. S. Ferekides, Thin Solid Films **515**, 6107 (2007).
[54] G. Fonthal, L. Tirado-Mejia, J. I. Marin-Hurtado, H. Ariza-Calderon, and J. G. Mendoza-Alvarez, J. Phys. Chem. Solids **61**, 579 (2000).

© 2016 WILEY-VCH Verlag GmbH & Co. KGaA, Weinheim

[55] S. Collins, S. Vatavu, V. Evani, M. Khan, S. Bakhshi, V. Palekis, C. Rotaru, and C. Ferekides, Thin Solid Films **582**, 139 (2015).
[56] H. S. Guder, B. Abay, H. Efeoglu, and Y. K. Yogurtcu, J. Lumin. **93**, 243 (2001).
[57] S. Vatavu, H. Zhao, Iu. Caraman, P. Gasin, and Ch. Ferekides, Thin Solid Films **519**, 7176 (2011).
[58] S. H. Song, J. F. Wang, G. M. Lalev, L. He, and M. Isshiki, J. Cryst. Growth **252**, 102 (2003).
[59] I. N. Odin, M. V. Chukichev, M. V. Gapanovich, and G. F. Novikov, Inorg. Mater. **47**, 588 (2011).
[60] X. Mathew, J. R. Arizmendi, J. Campos, P. J. Sebastian, N. R. Mathews, C. R. Jimenez, M. G. Jimenez, R. Silva-Gonzalez, M. E. Hernandez-Torres, and R. Dhere, Sol. Energy Mater. Sol. Cells **70**, 379 (2001).
[61] L. I. Grossweine, J. Appl. Phys. **24**, 1306 (1953).
[62] R. Chen and Y. Kirsh, Analysis of Thermally Stimulated Processes (Pergamon Press, Oxford, 1981).
[63] V. Pagonis, G. Kitis, and C. Furetta, Numerical and Practical Exercises in Thermoluminescence (Springer-Verlag, New York, 2006), p. 210.
[64] D. Pal, S. Pal, and D. N. Bose, Bull. Mater. Sci. **17**, 347 (1994).
[65] Y. Cui, D. D. Caudel, P. Bhattacharya, A. Burger, K. C. Mandal, D. Johnstone, and S. A. Payne, J. Appl. Phys. **105**, 053709 (2009).

© 2016 WILEY-VCH Verlag GmbH & Co. KGaA, Weinheim